

# Trivalent Aluminum Ionic Conduction in the Aluminum Tungstate–Scandium Tungstate–Lutetium Tungstate Solid Solution System

S. Tamura, T. Egawa, Y. Okazaki, Y. Kobayashi, N. Imanaka, and G. Adachi\*

Department of Applied Chemistry, Faculty of Engineering, Osaka University,  
2-1 Yamadaoka, Suita, Osaka 565-0871, Japan

Received March 2, 1998. Revised Manuscript Received May 15, 1998

The solid solutions of the  $\text{Al}_2(\text{WO}_4)_3$ – $\text{Sc}_2(\text{WO}_4)_3$ – $\text{Lu}_2(\text{WO}_4)_3$  series which hold the  $\text{Sc}_2(\text{WO}_4)_3$ -type structure were prepared and their ionic conducting characteristics were investigated. The maximum electrical conductivity was obtained for the solid solution of  $(\text{Al}_2(\text{WO}_4)_3)_{0.1}$ – $(\text{Sc}_{0.5}\text{Lu}_{0.5})_2(\text{WO}_4)_3)_{0.9}$ . By the measurements of the electrical conductivity dependencies on oxygen pressure and the polarization analyses, the mobile species in the solid solution was found to be only ionic and also oxide anion was eliminated from the candidates of the conducting ion species. Among the cation species in the solid solution, the mobile ion was demonstrated to be only  $\text{Al}^{3+}$  ion and the rest of the cations such as  $\text{Sc}^{3+}$ ,  $\text{Lu}^{3+}$ , and  $\text{W}^{6+}$  functioned as lattice-forming ions with oxide anion from the electrolysis experiments. Here, the highest  $\text{Al}^{3+}$  ion conduction was obtained in the  $\text{Sc}_2(\text{WO}_4)_3$ -type structure and the optimal lattice size for the  $\text{Al}^{3+}$  ion migration in the  $\text{Sc}_2(\text{WO}_4)_3$ -type structure was identified.

## Introduction

Mono- or divalent ionic motions in solid electrolytes are commonly known, and some of the solid electrolytes have already been applied practically in various fields such as industrial and biomedical areas.<sup>1</sup> In contrast, the idea that trivalent ions which possess a stronger interaction with the framework constituent like oxygen, are very poor migrant ions in solids has been generally accepted. Only a few papers have reported some probabilities of the trivalent cation conduction, e.g.,  $\text{Ln}^{3+}$ – $\beta''$ -alumina<sup>2–9</sup> and  $\beta$ - $\text{LaNbO}_3$ ,<sup>10</sup>  $\text{LaAl}_{11}\text{O}_{18}$ ,<sup>11</sup> and  $\text{LaAl}_{12}\text{O}_{18}\text{N}$ .<sup>11</sup> However, any direct and clear demonstration of the trivalent ion conduction in the solids has not been examined at all.

In these years, the trivalent ion conduction such as aluminum<sup>12</sup> and rare earth ions<sup>13,14</sup> has been directly and explicitly demonstrated. The suitable structure for

the trivalent ion conduction is the  $\text{Sc}_2(\text{WO}_4)_3$ -type structure<sup>15,16</sup> which holds a relatively larger ion migrating void to make the trivalent ion motion smoothly. In addition to this, one of the constituent elements, tungsten, makes a great contribution in obtaining the appropriate surroundings for the trivalent ions to conduct in the solid, since the W ion in the  $\text{Sc}_2(\text{WO}_4)_3$ -type structure exists in a hexavalent state and is strongly fixed to the constituent of divalent oxide anions. As a result of it, the trivalent ions in the  $\text{Sc}_2(\text{WO}_4)_3$ -type structure are left in such a circumstance to readily migrate in the tungstates.  $\text{Al}_2(\text{WO}_4)_3$  which is one of the tungstates to hold the  $\text{Sc}_2(\text{WO}_4)_3$ -type structure was quantitatively demonstrated to be an  $\text{Al}^{3+}$  ionic conductor with the ionic transference number of unity.<sup>12</sup> However, the  $\text{Al}^{3+}$  ionic conductivity of pure  $\text{Al}_2(\text{WO}_4)_3$  with the  $\text{Sc}_2(\text{WO}_4)_3$ -type structure is still low and the conductivity at 600 °C is 3 orders of magnitude lower compared with the representative oxide ionic conductors such as stabilized zirconias.<sup>17</sup> The  $\text{Sc}_2(\text{WO}_4)_3$ -type structure is a quasi-two-dimensional structure and the distance between layers can be changed by doping the trivalent ions with various ionic radius. We have already prepared the  $\text{Sc}_2(\text{WO}_4)_3$ – $\text{Lu}_2(\text{WO}_4)_3$ <sup>18</sup> and the  $\text{Sc}_2(\text{WO}_4)_3$ – $\text{Gd}_2(\text{WO}_4)_3$ <sup>19</sup> solid solutions with the  $\text{Sc}_2(\text{WO}_4)_3$ -type structure and clarified that the solid solutions are definitely the single phase and the lattice volume linearly depends on the average ionic size of the

(1) Adachi, G.; Imanaka, N. *Handbook on the Physics and Chemistry of Rare Earths*; North-Holland: Amsterdam, 1995; Vol. 21, p 179.

(2) Dunn, B.; Farrington, G. C. *Solid State Ionics* **1983**, 9/10, 223.

(3) Carrillo-Cabrera, W.; Thomas, J. O.; Farrington, G. C. *Solid State Ionics* **1983**, 9/10, 245.

(4) Ghosal, B.; Mangle, E. A.; Topp, M. R.; Dunn, B.; Farrington, G. C. *Solid State Ionics* **1983**, 9/10, 273.

(5) Farrington, G. C.; Dunn, B.; Thomas, J. O. *Appl. Phys.* **1983**, A32, 159.

(6) Dedecke, T.; Köhler, J.; Tietz, F.; Urland, W. *Eur. J. Solid State Inorg. Chem.* **1996**, 33, 185.

(7) Köhler, J.; Urland, W. *Solid State Ionics* **1996**, 86/88, 93.

(8) Köhler, J.; Balzer-Jöllenbeck, G.; Urland, W. *J. Solid State Chem.* **1996**, 122, 315.

(9) Köhler, J.; Urland, W. *Angew. Chem.* **1997**, 109, 105.

(10) George, A. M.; Virkar, A. N. *J. Phys. Chem. Solids* **1988**, 49, 743.

(11) Warner, T. E.; Fray, D. J.; Davies, A. *Solid State Ionics* **1996**, 92, 99.

(12) Kobayashi, Y.; Egawa, T.; Tamura, S.; Imanaka, N.; Adachi, G. *Chem. Mater.* **1997**, 9, 1649.

(13) Imanaka, N.; Kobayashi, Y.; Adachi, G. *Chem. Lett.* **1995**, 433.

(14) Imanaka, N.; Adachi, G. *J. Alloys Compds.* **1997**, 250, 492.

(15) Abrahams, S. C.; Bernstein, J. L. *J. Chem. Phys.* **1966**, 45, 2745.

(16) Nassau, K.; Levinstein, H. J.; Loiacono, G. M. *J. Phys. Chem. Solids* **1965**, 26, 1805.

(17) Etsell, T. H.; Flengas, S. N. *Chem. Rev.* **1970**, 70, 339.

(18) Kobayashi, Y.; Egawa, T.; Tamura, S.; Imanaka, N.; Adachi, G. *Solid State Ionics* In press.

(19) Kobayashi, Y.; Egawa, T.; Okazaki, Y.; Tamura, S.; Imanaka, N.; Adachi, G. *Solid State Ionics* In press.

trivalent ions in the individual solid solution series. In addition, the trivalent ion conduction in the above-mentioned two solid solutions are able to enhance the  $\text{Sc}^{3+}$  ionic conductivity approximately two and three times higher than that of pure  $\text{Sc}_2(\text{WO}_4)_3$ , respectively. In the above two solutions, the larger  $\text{Lu}^{3+}$  (0.1001 nm)<sup>20</sup> or  $\text{Gd}^{3+}$  (0.1078 nm)<sup>20</sup> ions compared with  $\text{Sc}^{3+}$  (0.0885 nm)<sup>20</sup> function to expand the  $\text{Sc}_2(\text{WO}_4)_3$  lattice size and resulted in the trivalent  $\text{Sc}^{3+}$  ion conductivity enhancement. By changing intentionally the ionic radius of the trivalent ions between the layers, an optimum crystal lattice for the mobile trivalent ion migration is achieved. Here, for the purpose of constructing the most suitable lattice for trivalent aluminum ion migration in the  $\text{Sc}_2(\text{WO}_4)_3$ -type structure, larger ions compared with aluminum (0.0675 nm)<sup>20</sup> such as scandium ion and one of the lanthanide ions, lutetium ion, which possesses further large ionic size compared with  $\text{Sc}^{3+}$  were selected as the lattice-forming trivalent ions in the structure.

In this investigation, the single  $\text{Sc}_2(\text{WO}_4)_3$ - $\text{Lu}_2(\text{WO}_4)_3$  solid solutions phases with various lattice size were prepared at first. Then, aluminum tungstate was further mixed to insert  $\text{Al}^{3+}$  ions between the layers of the tungstate of the various solid solutions and an optimal  $\text{Al}^{3+}$  ionic conductivity with the  $\text{Sc}_2(\text{WO}_4)_3$ -type structure and the optimum lattice size for the  $\text{Al}^{3+}$  ionic migration in the structure were quantitatively determined.

### Experimental Section

**Sample Preparation.** At first, solid solutions of the  $(1-x)\text{Sc}_2(\text{WO}_4)_3-x\text{Lu}_2(\text{WO}_4)_3$  system were prepared by a conventional solid state reaction. An appropriate amount of reagent grade  $\text{Sc}_2\text{O}_3$  (purity 99.9%),  $\text{Lu}_2\text{O}_3$  (purity 99.9%), and  $\text{WO}_3$  (purity 99.9%) was mixed in an agate mortar and calcined at 1000 °C for 12 h in air and then heat treated at 1200 °C for 12 h in the same atmosphere. The sample characterization was done by X-ray powder diffraction using  $\text{Cu K}\alpha$  radiation (M18XHF, Mac Science). The XRD data were collected by a step-scanning method for the  $2\theta$  range between 10° and 120° with a step width of 0.02° and a scan time of 4 s. The X-ray patterns obtained were analyzed by the Rietveld refinement program, RIETAN-94,<sup>21</sup> and the cell parameters of the solid solutions were precisely determined.  $\text{Al}_2(\text{WO}_4)_3$  was prepared by firing the mixture of  $\text{Al}(\text{OH})_3$  and  $\text{WO}_3$  at 1000 °C until the color of the powder became white. The resulting powder of the  $(\text{Sc}, \text{Lu})_2(\text{WO}_4)_3$  solid solution was further mixed with the  $\text{Al}_2(\text{WO}_4)_3$  powder and made into pellets (10 mm in diameter and ca. 0.8 mm in thickness). The pellets were heated at 1100 °C for 12 h and then sintered at 1200 °C for 12 h in air.

**Measurements.** The electrical conductivity of the samples was measured by a complex impedance method at the frequency range from 20 Hz to 1 MHz (Precision LCR meter 8284A, Hewlett Packard) in the temperature range from 200 to 600 °C, using the sintered pellet with a Pt sputtered electrode on both surface. The constant current of 0.1  $\mu\text{A}$  was passed between the two Pt electrodes sandwiching the sample, and the voltage was monitored as a function of time. The DC conductivity was obtained by the calculation from the voltage, the applied current, the surface area, and the thickness of the sample.

For the purpose of determining the charge carrier in the solid solutions, the DC electrolysis was performed with two platinum plates as the electrode by applying a voltage of 1 V

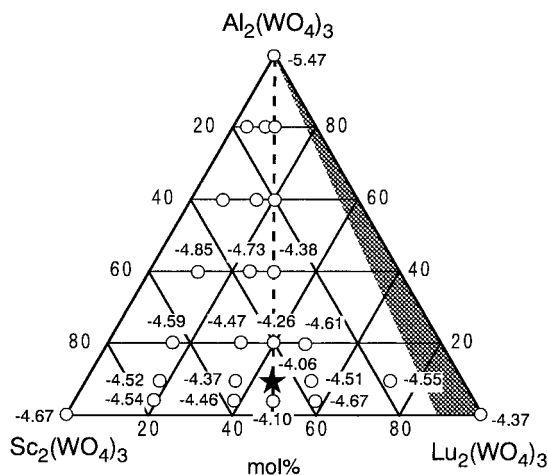


**Figure 1.** Relationship between the electrical conductivities in the  $\log \sigma$  expression and the compositions of the  $\text{Al}_2(\text{WO}_4)_3$ - $\text{Sc}_2(\text{WO}_4)_3$ - $\text{Lu}_2(\text{WO}_4)_3$  system at 600 °C.

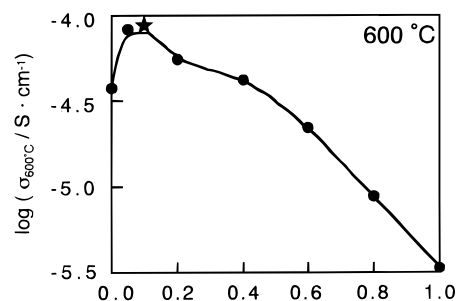


**Figure 2.** Al content dependencies of the conductivities for  $(\text{Al}_2(\text{WO}_4)_3)_x-(\text{Sc}_{0.5}\text{Lu}_{0.5})_2(\text{WO}_4)_3(1-x)$  at 600 °C.

for 250 h at 900 °C in air. After the electrolysis, scanning electron microscope (SEM, S-800, HITACHI) measurements and electron probe microanalysis (EPMA-1500, Shimadzu) were carried out for the cathodic bulk surface and the inside of the bulk.

### Results and Discussion

The lattice parameters of  $a$ ,  $b$ , and  $c$  increased monotonically by substituting the scandium site in  $\text{Sc}_2(\text{WO}_4)_3$  with the larger lutetium ion.<sup>18</sup> With the increase of the lattice size, the electrical conductivity was linearly enhanced with the Lu replacement until  $x = 0.5$  in  $(\text{Sc}_{1-x}\text{Lu}_x)_2(\text{WO}_4)_3$ . On the other hand, the ionic conductivity was reduced when the Lu site in  $\text{Lu}_2(\text{WO}_4)_3$  was substituted with  $\text{Sc}^{3+}$ , up to 40 mol %. A discontinuity appeared in the relationship between the ionic conductivity and the composition of the solid solution approximately 50–60 Lu mol % replacement of the Sc site in the  $\text{Sc}_2(\text{WO}_4)_3$ -type structure. The solid solution was found to be a  $\text{Sc}^{3+}$  and  $\text{Lu}^{3+}$  mixed ionic conductor, and the predominant conducting species were clarified to be  $\text{Sc}^{3+}$  and  $\text{Lu}^{3+}$  below and above the 50–60 Lu mol % substitution. There is a close relationship between the lattice volume and the ionic conductivity of the individual mobile trivalent ion,  $\text{Sc}^{3+}$  and  $\text{Lu}^{3+}$ .

The target in this research is to obtain a superior  $\text{Al}^{3+}$  ion conducting solid electrolyte with the  $\text{Sc}_2(\text{WO}_4)_3$ -type solid solution by adjusting the lattice size optimal with the several different size of trivalent cations. For this

(20) Shannon, R. D. *Acta Crystallogr.* **1976**, *A32*, 751.

(21) Izumi, F. *The Rietveld Method*; Oxford University Press: Oxford, 1993, Chapter 13.

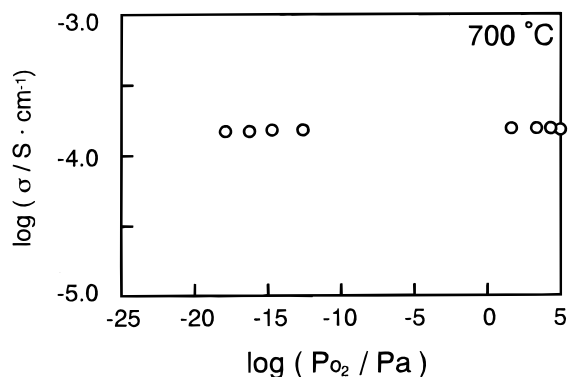


**Figure 3.** Oxygen pressure dependencies of the electrical conductivity for  $(\text{Al}_2(\text{WO}_4)_3)_{0.1}-((\text{Sc}_{0.5}\text{Lu}_{0.5})_2(\text{WO}_4)_3)_{0.9}$  at  $700\text{ }^\circ\text{C}$ .

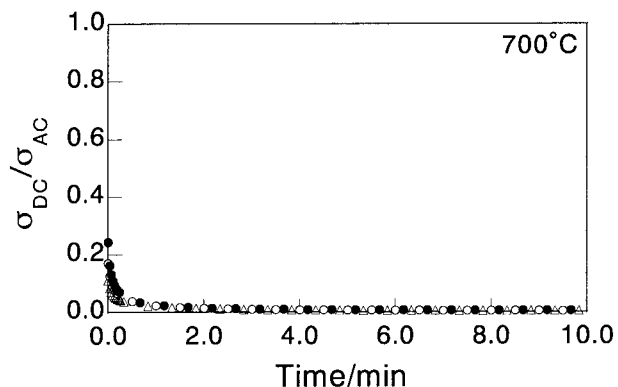


**Figure 4.** Polarization behavior ( $\sigma_{\text{DC}}/\sigma_{\text{AC}}$ ) for  $(\text{Al}_2(\text{WO}_4)_3)_{0.1}-((\text{Sc}_{0.5}\text{Lu}_{0.5})_2(\text{WO}_4)_3)_{0.9}$  in oxygen ( $10^5\text{ Pa}$ ) (●), nitrogen ( $10^2\text{ Pa}$ ) (○), and helium ( $1\text{ Pa}$ ) (△) atmospheres at  $700\text{ }^\circ\text{C}$ .

purpose,  $\text{Al}^{3+}$  ions are further inserted between the layers of  $(\text{Sc}, \text{Lu})_2(\text{WO}_4)_3$  solid solutions.

Figure 1 presents the triangular diagram of the electrical conductivity for the  $\text{Al}_2(\text{WO}_4)_3-\text{Sc}_2(\text{WO}_4)_3-$

$\text{Lu}_2(\text{WO}_4)_3$  system at  $600\text{ }^\circ\text{C}$ . The complete single phase of the  $\text{Sc}_2(\text{WO}_4)_3$ -type solid solution was obtained except for the shadow region of the two-phase mixture of the  $\text{Al}_2(\text{WO}_4)_3$  single phase and the  $(\text{Sc}, \text{Lu})_2(\text{WO}_4)_3$  solid solution. The values indicated in the figure are the logarithm of the measured electrical conductivity. Among the solutions investigated, the  $(\text{Al}_2(\text{WO}_4)_3)_{0.1}-((\text{Sc}_{0.5}\text{Lu}_{0.5})_2(\text{WO}_4)_3)_{0.9}$  solid solution shows the highest electrical conductivity of  $-4.06$  in the  $\log \sigma$  expression.

Figure 2 shows the  $\text{Al}^{3+}$  content dependencies of the electrical conductivity of the line which contains the highest value of  $-4.06$  and the value of  $-5.47$  for pure  $\text{Al}_2(\text{WO}_4)_3$  in  $\log \sigma$  as indicated in a break line in Figure 1. From the figure, it can be easily recognized that the maximum electrical conductivity was attained for the  $\text{Al}_2(\text{WO}_4)_3$  and  $(\text{Sc}_{0.5}\text{Lu}_{0.5})_2(\text{WO}_4)_3$  ratio of 1:9 in the  $(\text{Al}, \text{Sc}, \text{Lu})_2(\text{WO}_4)_3$  solid solution series and the conductivity is approximately 25 times higher than that of pure  $\text{Al}_2(\text{WO}_4)_3$ .

The oxygen pressure dependencies of the electrical conductivity for the  $(\text{Al}_2(\text{WO}_4)_3)_{0.1}-((\text{Sc}_{0.5}\text{Lu}_{0.5})_2(\text{WO}_4)_3)_{0.9}$  solid solution at  $700\text{ }^\circ\text{C}$  is depicted in Figure 3. In the whole oxygen pressure region measured ( $10^5\text{ Pa}$  to  $10^{-18}\text{ Pa}$ ), the conductivity was constant in the  $\log \sigma-\log P_{\text{O}_2}$  relation. The solid solution was found to be stable in such a wide oxygen pressure range. This phenomenon clearly indicates that any hole or electron conduction does not appear in the  $(\text{Al}_2(\text{WO}_4)_3)_{0.1}-((\text{Sc}_{0.5}\text{Lu}_{0.5})_2(\text{WO}_4)_3)_{0.9}$  solid solution, and the solution was clarified to show predominantly ionic conducting characteristics.

The polarization measurements were carried out in helium ( $1\text{ Pa}$ ), nitrogen ( $10^2\text{ Pa}$ ), and oxygen ( $10^5\text{ Pa}$ ) at  $700\text{ }^\circ\text{C}$ , and the results are presented in Figure 4. The DC to AC conductivity ratio,  $\sigma_{\text{DC}}/\sigma_{\text{AC}}$ , abruptly decreased and held a steady state after 5 min. A clear polarization was similarly observed in the three differ-

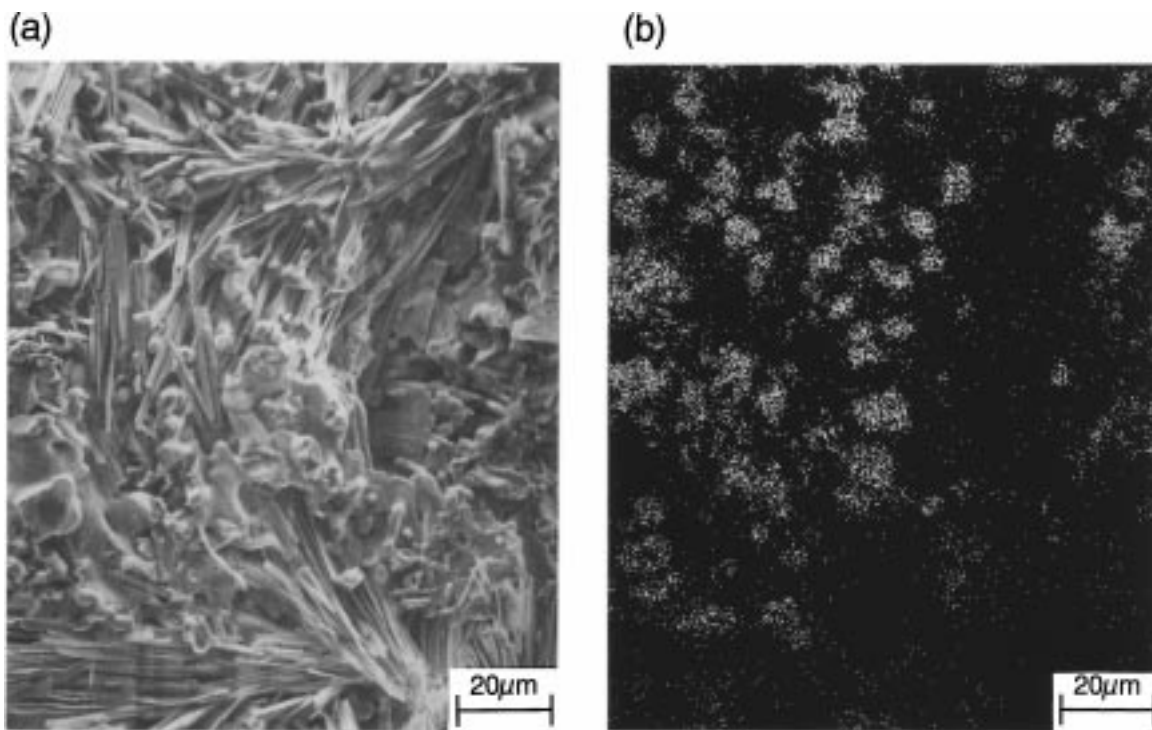


**Figure 5.** (a) SEM photograph and (b) the Al distribution in the photo at the cathodic surface of  $(\text{Al}_2(\text{WO}_4)_3)_{0.1}-((\text{Sc}_{0.5}\text{Lu}_{0.5})_2(\text{WO}_4)_3)_{0.9}$  after the electrolysis.



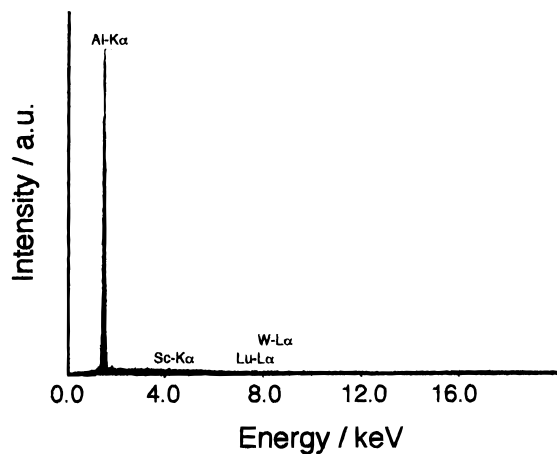


**Figure 6.** EPMA point analysis of the clusters of ball shape deposits in Figure 5a.

ent gas atmospheres, and the  $\sigma_{DC}/\sigma_{AC}$  value decreased more than 3 orders of magnitude. This high polarization behavior tells us that the ionic transference number is over 0.999. In the solid solutions, ionic species contained are trivalent aluminum and rare earth ions, hexavalent tungsten ion, and divalent oxide anion. However, even in the oxygen atmosphere, an abrupt decrease in  $\sigma_{DC}/\sigma_{AC}$  was also similarly observed. If the solid solution is an oxide ion conductor, no polarization is observed in the oxygen atmosphere, while a clear polarization behavior appears in helium as described in our previous paper.<sup>12</sup> The phenomena observed in Figure 4 definitely indicate that the oxide ion is not a mobile ion species in the solid solution.

The SEM photograph and the Al distribution in the photo obtained by the EPMA measurements are shown in Figures 5a and 5b. A lot of clusters of ball shape deposits were observed, and the element detected by EPMA is only aluminum in the clusters without any Sc, Lu, and W existence as presented in Figure 6.

The cross-sectional EPMA line analysis for the  $(Al_2(WO_4)_3)_{0.1} - ((Sc_{0.5}Lu_{0.5})_2(WO_4)_3)_{0.9}$  solid solution is presented in Figure 7. Since the DC electrolysis was conducted for about 250 h, the mobile cationic species was in such a circumstance as to be forced to migrate from the anodic to the cathodic direction. The Sc, Lu, and W elements were found to be equally distributed from the cross-sectional line analysis of the pellet. On the contrary, a considerable  $Al^{3+}$  segregation appeared on the cathodic surface. These results mean that the  $Al^{3+}$  ion migration is much smoother than the ionic migrations of  $Sc^{3+}$ ,  $Lu^{3+}$ , and also  $W^{6+}$  in the  $Sc_2(WO_4)_3$ -type structure. The above-mentioned SEM and EPMA results explicitly indicate that the predominant mobile ionic species was demonstrated to be only  $Al^{3+}$  in the four mobile ion candidates such as  $Al^{3+}$ ,  $Sc^{3+}$ ,  $Lu^{3+}$ , and  $W^{6+}$  in the solid solution.

Figure 8 depicts the temperature dependencies of the  $Al^{3+}$  ionic conductivity for the  $(Al_2(WO_4)_3)_{0.1} - ((Sc_{0.5}Lu_{0.5})_2(WO_4)_3)_{0.9}$  solid solution with the data of pure  $Al_2(WO_4)_3$  solid electrolyte previously reported.<sup>12</sup> The  $Al^{3+}$  ionic conductivity increased about 25 times higher than that of pure  $Al_2(WO_4)_3$ . In addition, the activation energy for the solid solution and pure  $Al_2(WO_4)_3$  are 61.8 kJ/mol and 93.6 kJ/mol, respectively. By expanding the lattice size in an optimum volume for the  $Al^{3+}$  ion

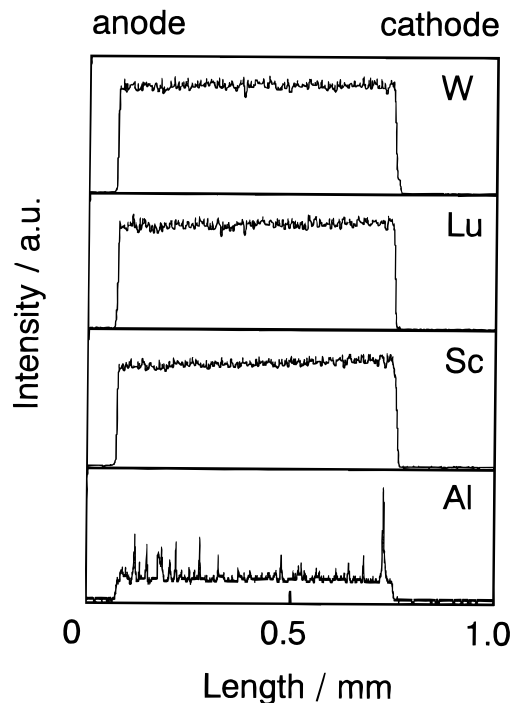


**Figure 7.** Cross-sectional EPMA line analysis for  $(Al_2(WO_4)_3)_{0.1} - ((Sc_{0.5}Lu_{0.5})_2(WO_4)_3)_{0.9}$  solid solution after the electrolysis.

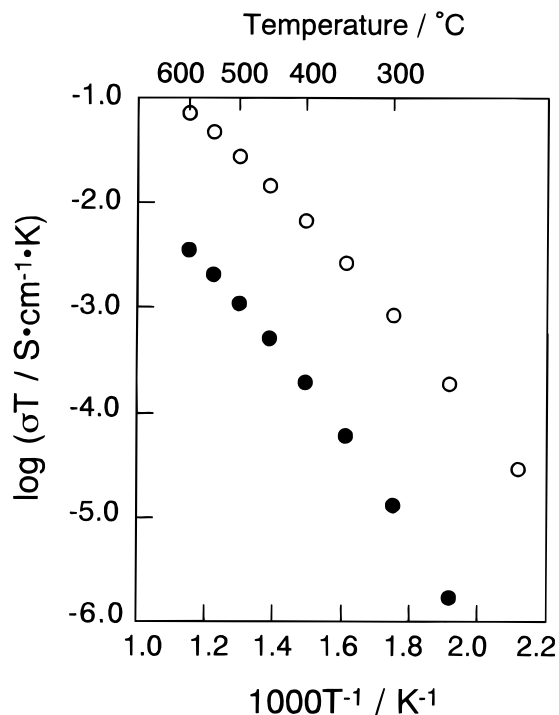


**Figure 8.** Temperature dependencies of the  $Al^{3+}$  ionic conductivity for  $(Al_2(WO_4)_3)_{0.1} - ((Sc_{0.5}Lu_{0.5})_2(WO_4)_3)_{0.9}$  solid solution (O) and for pure  $Al_2(WO_4)_3$  (●).

migration in the  $Sc_2(WO_4)_3$ -type solid solution, the activation energy ( $E_a$ ) for the  $Al^{3+}$  ionic conduction becomes lower than that of pure  $Al_2(WO_4)_3$  and the  $E_a$  is exactly the lowest value for the  $Al^{3+}$  ion conduction in the  $Sc_2(WO_4)_3$ -type structure. Figure 8 clearly gives us the fact that by choosing the most suitable lattice size for the  $Al^{3+}$  ion migration in the  $Sc_2(WO_4)_3$ -type structure, the  $Al^{3+}$  ionic conduction in the tungstate structure is intentionally enhanced and optimized com-

pared with the nominal solid electrolyte of pure  $\text{Al}_2(\text{WO}_4)_3$ .

**Acknowledgment.** We thank Dr. K. Yamada for EPMA measurements and for helpful discussions. The present work was partially supported by a Grant-in-Aid for Scientific Research No. 09215223 on Priority Areas (No. 260), Nos. 06241106, 06241107, and 093065

from The Ministry of Education, Science, Sports and Culture. This work was also supported by the Research for the Future, Preparation and Application of Newly Designed Solid Electrolytes (JSPS-RFTF96P00102) Program from the Japan Society for the Promotion of Science.

CM980115Q